Index-3 divide and conquer algorithm for efficient multibody dynamics simulations

Paweł Malczyk[1], Janusz Frączek[1], Francisco González[2], Javier Cuadrado[2]

[1] Institute of Aeronautics and Applied Mechanics
Faculty of Power and Aeronautical Engineering
Warsaw University of Technology
Nowowiejska 24, 00-665 Warsaw, Poland
[pmalczyk,jfraczek]@meil.pw.edu.pl

[2] Laboratorio de Ingeniería Mecánica
Escuela Politecnica Superior
University of La Coruña
Mendizábal s/n, 15403 Ferrol, Spain
[f.gonzalez,javicuad]@cdf.udc.es

Abstract

There has been a growing attention to efficient simulations of multibody systems. This trend is apparently seen in many areas of computer aided engineering and design both in academia as well as in industry (e.g. in industrial or space robotics, in automotive industry or in a variety of simulators for mining, construction or crane operations including cables and ropes simulations). The need for efficient or real-time simulations require better and faster formulations. Parallel computing is one of the approaches to achieve this objective. This paper presents a novel divide and conquer algorithm for efficient multibody dynamics simulations. A redundant set of absolute coordinates is used for the system state description. The trapezoidal rule is exploited as a numerical integrator. Sample multibody system test cases are reported in the paper to indicate overall characteristics of the formulation measured in terms of constraint violation errors and total energy conservation. The gathered data indicate good performance indices of the formulation with the prospect for efficient or real-time simulations of complex multibody systems in parallel computing environments.

Keywords: divide and conquer algorithm, multibody dynamics, real-time simulations, mass-orthogonal projections

1. Introduction

Computational efficiency has traditionally been a major concern of researchers developing algorithms for multibody dynamics simulations. Considerable improvements in computer architectures have taken place during the last years, enabling the efficient simulation of larger and more complex mechanical systems. Also the expectations about the performance that a multibody software tool can deliver have grown at the same pace.

The availability of distributed computing environments and parallel architectures, equipped with inexpensive multi-core processors and graphical processor units, has encouraged researchers to develop parallel multibody dynamics algorithms [1]. Featherstone's Divide and Conquer Algorithm (DCA) [2] is among the most popular ones. Its binary-tree structure allows distributing the computations among several processing cores in a scalable and relatively simple way. In open chains with n bodies it can achieve $O\left(\log\left(n\right)\right)$ performance if enough processors are available [3]. The DCA constitutes the building block of dozens of methods and parallel codes for multibody dynamics [4]. Some of these introduced changes in the way originally proposed to deal with closed kinematic loops [5] and other constraints [6]. Others extended the algorithm to enable the consideration of flexible bodies [3], [7], discontinuities in system definition [8], and contacts [9]. Computational improvements to the initial algorithm have been published as well, such as techniques to keep constraint drift under control [10, 11] and optimized variants for computer architectures with reduced computational power [12]. The practical applications of the DCA are multiple and range from the simulation of simple linkages and multibody chains to molecular dynamics [13, 14].

The DCA scheme does not specify the way in which the system equations of motion must be formulated and several approaches can be followed to do this. A spatial formulation of the Newton-Euler equations was used in the initial definition of the algorithm and subsequently adopted by many of the formalisms that were derived from it, e.g., [5], [12]. However, other expressions of the dynamics equations can be used as well. The Articulated Body Algorithm (ABA) [15] was combined with the DCA in [16] to deliver significant speedups in computation times. Hamilton's canonical equations were used in [17, 18] and showed good properties regarding the satisfaction of kinematic constraints. Augmented Lagrangian methods with configuration- and velocity-level mass-orthogonal projections have also been employed [19]; the resulting algorithm has been proven to behave robustly during the simulation of mechanical systems with redundant constraints and singular configurations.

Augmented Lagrangian methods are common in multibody literature. Many of them were derived from the penalty formulation in [20], in which the constraint reactions were made proportional to the violation of kinematic constraints at the configuration, velocity, and acceleration levels. An augmented Lagrangian algorithm was also proposed in [20]

that complemented the penalty formulation with a set of modified Lagrange multipliers, evaluated iteratively, to satisfy more accurately the kinematic constraints and obtain stable and precise simulations for wider ranges of penalty factors. Mass-orthogonal projections were introduced in [21] to ensure the satisfaction of the constraints down to machine-precision levels. An index-3 algorithm, in which the dynamics equations were combined with the Newmark integration formulas to produce an iterative method in Newton-Raphson form was described in [21] as well. Such method was later improved to deliver real-time performance in [22] and [23], and to handle nonholonomic constraints in [24]. This index-3 augmented Lagrangian algorithm with projections of velocities and accelerations (ALi3p) has shown very good efficiency and robustness in the simulation of multibody systems in real-time industrial applications, e.g. [25].

The ALi3p and the DCA were first combined for the simulation of open-loop chains in [26]. In this work we continue this avenue and propose a novel and generalized index-3 divide and conquer formulation for multi-rigid body dynamics that elegantly handles potential numerical difficulties found in such simulations.

2. Equations of motion for constrained spatial systems

Before embarking on the divide and conquer formulation, the general form of the equations of motion for constrained spatial multibody system (MBS) is recalled. The system dynamics is formulated in terms of a set of absolute coordinates involving Euler parameters. Consider n bodies that form a multibody system (MBS). The composite set of generalized coordinates for the system is $\mathbf{q} = \begin{bmatrix} \mathbf{q}_1^T & \mathbf{q}_2^T & \cdots & \mathbf{q}_n^T \end{bmatrix}^T$, where $\mathbf{q}$ contains the absolute coordinates of all of the bodies in the system. For a particular body i the absolute coordinates can be written as $\mathbf{q}_i = \begin{bmatrix} \mathbf{r}_i^T, \mathbf{p}_i^T \end{bmatrix}^T$, $i = 1, \cdots, n$, where $\mathbf{r}_i = \begin{bmatrix} x_i & y_i & z_i \end{bmatrix}^T$ refers to the global Cartesian coordinates (i.e. expressed with respect to the global coordinate frame $(x_0 y_0 z_0)$) of the body-fixed centroidal coordinate frame $(x_i y_i z_i)$ and $\mathbf{p}_i = \begin{bmatrix} e_{0i} & e_{1i} & e_{2i} & e_{3i} \end{bmatrix}^T = \begin{bmatrix} e_{0i} & \mathbf{e}_i^T \end{bmatrix}^T$ corresponds to the set of four Euler parameters that describe the orientation of body i with respect to the global reference frame $(x_0 y_0 z_0)$. Rigid bodies in MBS are interconnected by l joints. It is assumed that there are m holonomic constraint equations that relate the absolute coordinates as follows

$$\boldsymbol{\Phi}(\mathbf{q}) = \begin{bmatrix} \boldsymbol{\Phi}_1^T, \boldsymbol{\Phi}_2^T, \cdots, \boldsymbol{\Phi}_l^T \end{bmatrix}^T = \mathbf{0}_{m \times 1}. \tag{1}$$

In the following derivations, there is a necessity to evaluate first and second time derivatives of constraint conditions shown in Eqn. (1). The velocity and acceleration constraint equations can be expressed as

$$\dot{\boldsymbol{\Phi}} \equiv \boldsymbol{\Phi}_{\mathbf{q}} \dot{\mathbf{q}} = \mathbf{0}_{m \times 1}, \tag{2}$$

$$\ddot{\boldsymbol{\Phi}} \equiv \boldsymbol{\Phi}_{\mathbf{q}} \ddot{\mathbf{q}} + \dot{\boldsymbol{\Phi}}_{\mathbf{q}} \dot{\mathbf{q}} = \boldsymbol{\Phi}_{\mathbf{q}} \ddot{\mathbf{q}} - \boldsymbol{\gamma} = \mathbf{0}_{m \times 1}, \tag{3}$$

where $\boldsymbol{\Phi}_{\mathbf{q}}$ is the constraint Jacobian matrix. In addition, the Euler parameter normalization constraints must hold. There are n such conditions in the form

$$\Psi_i(\mathbf{q}_i) = \mathbf{p}_i^T \mathbf{p}_i - 1 = 0. \tag{4}$$

Similarly to Eqn. (2) and Eqn. (3), one can define the velocity constraints $\dot{\Psi}_i = 0$ and acceleration level conditions $\ddot{\Psi}_i = 0$. Let us define the following matrix for body i

$$\mathbf{M}_i = \begin{bmatrix} m_i \mathbf{I}_{3 \times 3} & \mathbf{0} \\ \mathbf{0} & 4\mathbf{G}_i^T \mathbf{J}_i' \mathbf{G}_i \end{bmatrix}, \quad i = 1, \cdots, n, \tag{5}$$

where m_i is the mass of body i, $\mathbf{J}_i'$ is the inertia matrix expressed with respect to centroidal coordinate frame $(x_i y_i z_i)$, and $\mathbf{G}_i = \begin{bmatrix} -\mathbf{e}_i, & -\tilde{\mathbf{e}}_i + e_{0i} \mathbf{I}_{3 \times 3} \end{bmatrix}$ is a useful 3×4 matrix that involves Euler parameters that fulfills the relation $\boldsymbol{\omega}_i' = 2\mathbf{G}_i \dot{\mathbf{p}}_i$ ($\boldsymbol{\omega}_i'$ – angular velocity of body i expressed in the local coordinate frame). The vector of generalized forces acting on body i is

$$\mathbf{Q}_i = \begin{bmatrix} \mathbf{f}_i \\ 2\mathbf{G}_i^T \mathbf{n}_i' - 8\dot{\mathbf{G}}_i^T \mathbf{J}_i' \mathbf{G}_i \end{bmatrix}, \quad i = 1, \cdots, n. \tag{6}$$

The active forces $\mathbf{f}_i$ acting on body i are expressed in the global reference frame $(x_0 y_0 z_0)$, whereas active torques $\mathbf{n}_i'$ are expressed in the body-fixed centroidal coordinate frame. Finally, the Euler parameter form of constrained equations of motion for spatial multibody system can be expressed as

$$\begin{bmatrix} \mathbf{M} & \boldsymbol{\Phi}_{\mathbf{q}}^T & \boldsymbol{\Psi}_{\mathbf{q}}^T \\ \boldsymbol{\Phi}_{\mathbf{q}} & & \mathbf{0} \\ \boldsymbol{\Psi}_{\mathbf{q}} & & \end{bmatrix} \begin{bmatrix} \ddot{\mathbf{q}} \\ \boldsymbol{\lambda} \\ \boldsymbol{\mu} \end{bmatrix} = \begin{bmatrix} \mathbf{Q} \\ \boldsymbol{\gamma} \\ \boldsymbol{\eta} \end{bmatrix} \tag{7}$$
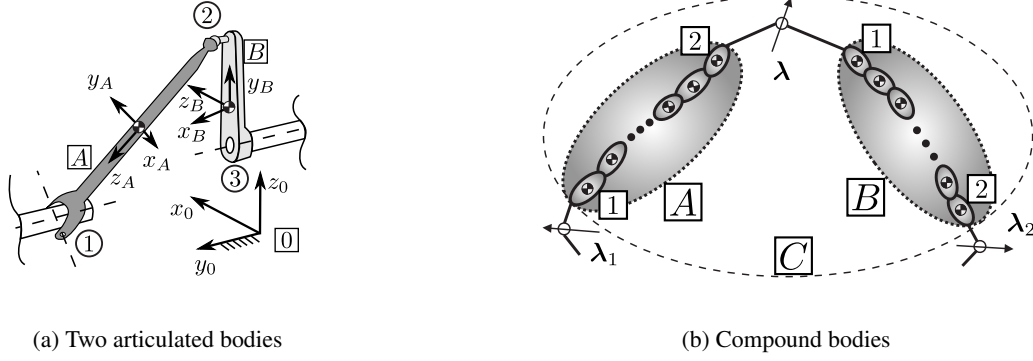
(a) Two articulated bodies   (b) Compound bodies

Figure 1: Two articulated bodies and generalization in the form of compound bodies

with the addition of the following definitions

$$\mathbf{M} = diag(\mathbf{M}_1, \cdots, \mathbf{M}_n), \quad \mathbf{Q} = \left[\mathbf{Q}_1^T, \cdots, \mathbf{Q}_n^T\right]^T. \tag{8}$$

Moreover, the vector of Lagrange multipliers $\boldsymbol{\lambda}$ that corresponds to constraint reactions at joints and the vector of Lagrange multipliers $\boldsymbol{\mu}$ associated with Euler normalization constraints are given as

$$\boldsymbol{\lambda} = \left[\boldsymbol{\lambda}_1^T, \boldsymbol{\lambda}_2^T, \cdots, \boldsymbol{\lambda}_l^T\right]_{m \times 1}^T, \quad \boldsymbol{\mu} = \left[\mu_1, \mu_2, \cdots, \mu_n\right]_{n \times 1}^T. \tag{9}$$

In the following sections the form of constrained equations of motion presented in Eqn. (7) will be heavily exploited to explain the details of the divide and conquer based formulation.

3. Algorithm formulation

3.1. Two articulated rigid bodies

This subsection will serve as an introduction to the derivation of the divide and conquer based formulation proposed in this paper. Specifically, consider two representative bodies A and B demonstrated in Fig. 1a. The bodies are connected to each other by joint 2 and form only a part of the whole multibody system. Body A and body B are also connected to the rest of multibody system by joint 1 and joint 3, respectively.

Equations of motion for constrained bodies A and B can be written similarly as in Eqn. (7). For convienience, we define two functions $\mathbf{g}_A$ and $\mathbf{g}_B$, to get

$$\mathbf{g}_A \equiv \mathbf{M}_A \ddot{\mathbf{q}}_A + \mathbf{F}_A^1 + \mathbf{F}_A^2 + \Psi_{A\mathbf{q}_A}^T \mu_A - \mathbf{Q}_A = \mathbf{0}, \tag{10}$$

$$\mathbf{g}_B \equiv \mathbf{M}_B \ddot{\mathbf{q}}_B + \mathbf{F}_B^2 + \mathbf{F}_B^3 + \Psi_{B\mathbf{q}_B}^T \mu_B - \mathbf{Q}_B = \mathbf{0}, \tag{11}$$

where $\mathbf{F}_A^1$, $\mathbf{F}_A^2$ are constraint reactions at joints 1 and 2, which are acting on body A, whereas the vectors $\mathbf{F}_B^2$, $\mathbf{F}_B^3$ correspond to constraint forces at joint 2 and 3 that are acting on body B. Moreover, the following conditions are held

$$\mathbf{F}_A^1 = \Phi_{\mathbf{q}_A}^{1T} \boldsymbol{\lambda}_1, \ \mathbf{F}_A^2 = \Phi_{\mathbf{q}_A}^{2T} \boldsymbol{\lambda}_2, \ \mathbf{F}_B^2 = \Phi_{\mathbf{q}_B}^{2T} \boldsymbol{\lambda}_2, \ \mathbf{F}_B^3 = \Phi_{\mathbf{q}_B}^{3T} \boldsymbol{\lambda}_3. \tag{12}$$

Let us also note that the equivalent mass matrices $\mathbf{M}_A$, $\mathbf{M}_B$ of size 7×7 in Eqn. (10) and Eqn. (11) are singular. This issue is particularly inconvenient when one would like to apply the divide and conquer method. Later in this section this problem will be alleviated by proper use of the penalty method.

In this work the equations of motion for constrained multibody system will be integrated by single-step trapezoidal rule. This integration scheme has been adopted for the simulation due to its good numerical properties. The difference equations in velocities and accelerations can be written as

$$\dot{\mathbf{q}} = \frac{2}{\Delta t}\mathbf{q} + \hat{\dot{\mathbf{q}}}, \quad \text{where} \quad \hat{\dot{\mathbf{q}}} = -\left(\frac{2}{\Delta t}\overline{\mathbf{q}} + \dot{\overline{\mathbf{q}}}\right), \quad \text{and} \quad \ddot{\mathbf{q}} = \frac{4}{\Delta t^2}\mathbf{q} + \hat{\ddot{\mathbf{q}}}, \quad \text{where} \quad \hat{\ddot{\mathbf{q}}} = -\left(\frac{4}{\Delta t^2}\overline{\mathbf{q}} + \frac{4}{\Delta t}\dot{\overline{\mathbf{q}}} + \ddot{\overline{\mathbf{q}}}\right) \tag{13}$$

Please note that subscripts indicating the time instant have been omitted. It is assumed that $\mathbf{q}_{k+1} \equiv \mathbf{q}$ (next time-instant) and $\mathbf{q}_k \equiv \overline{\mathbf{q}}$ (current time-instant), where k is the index associated with arbitrary k^{th} time-instant. Now, let us introduce

Eqn. (13) into Eqn. (10) and Eqn. (11) at the next time step. After scaling the resulting equations by $\frac{\Delta t^2}{4}$, we get

$$\mathbf{M}_A \mathbf{q}_A + \frac{\Delta t^2}{4} \left(\mathbf{F}_A^1 + \mathbf{F}_A^2 + \Psi_{A\mathbf{q}_A}^T \mu_A - \mathbf{Q}_A + \mathbf{M}_A \hat{\ddot{\mathbf{q}}}_A \right) = \mathbf{0}, \tag{14}$$

$$\mathbf{M}_B \mathbf{q}_B + \frac{\Delta t^2}{4} \left(\mathbf{F}_B^2 + \mathbf{F}_B^3 + \Psi_{B\mathbf{q}_B}^T \mu_B - \mathbf{Q}_B + \mathbf{M}_B \hat{\ddot{\mathbf{q}}}_B \right) = \mathbf{0}. \tag{15}$$

Algebraic relations (14) and (15) constitute a discretized form of equations of motion (10) and (11) expressed at the next time-instant. They also form a system of nonlinear equations in positions $\mathbf{q}_A$, $\mathbf{q}_B$ and Lagrange multipliers. These equations may be solved by using the Newton-Raphson procedure. The position vector $\overline{\mathbf{q}}$ and Lagrange multipliers $\overline{\lambda}$, $\overline{\mu}$ at the current time instant are taken as initial guesses. Following this idea one can obtain the system of linear equations in the form:

$$\check{\mathbf{M}}_A \Delta \mathbf{q}_A + \frac{\Delta t^2}{4} \left(\Delta \mathbf{F}_A^1 + \Delta \mathbf{F}_A^2 + \Psi_{A\mathbf{q}_A}^T \Delta \mu_A \right) = -\frac{\Delta t^2}{4} \mathbf{g}_A, \tag{16}$$

$$\check{\mathbf{M}}_B \Delta \mathbf{q}_B + \frac{\Delta t^2}{4} \left(\Delta \mathbf{F}_B^2 + \Delta \mathbf{F}_B^3 + \Psi_{A\mathbf{q}_B}^T \Delta \mu_B \right) = -\frac{\Delta t^2}{4} \mathbf{g}_B, \tag{17}$$

where $\check{\mathbf{M}}_A = \mathbf{M}_A - \frac{\Delta t}{2} \frac{\partial \mathbf{Q}_A}{\partial \mathbf{q}_A} - \frac{\Delta t^2}{4} \frac{\partial \mathbf{Q}_A}{\partial \dot{\mathbf{q}}_A}$, $\check{\mathbf{M}}_B = \mathbf{M}_B - \frac{\Delta t}{2} \frac{\partial \mathbf{Q}_B}{\partial \mathbf{q}_B} - \frac{\Delta t^2}{4} \frac{\partial \mathbf{Q}_B}{\partial \dot{\mathbf{q}}_B}$ are equivalent mass matrices, vectors $\Delta \mathbf{q}_A = \mathbf{q}_A - \overline{\mathbf{q}}_A$, $\Delta \mathbf{q}_B = \mathbf{q}_B - \overline{\mathbf{q}}_B$ denote the increments in positions. In turn, vectors $\Delta \lambda_1 = \lambda_1 - \overline{\lambda}_1$, $\Delta \lambda_2 = \lambda_2 - \overline{\lambda}_2$, $\Delta \lambda_3 = \lambda_3 - \overline{\lambda}_3$ are used to define the increments in constraint forces $\Delta \mathbf{F}_A^1 = \Phi_{\mathbf{q}_A}^{1T} \Delta \lambda_1$, $\Delta \mathbf{F}_A^2 = \Phi_{\mathbf{q}_A}^{2T} \Delta \lambda_2$, and $\Delta \mathbf{F}_B^2 = \Phi_{\mathbf{q}_B}^{2T} \Delta \lambda_2$, $\Delta \mathbf{F}_B^3 = \Phi_{\mathbf{q}_B}^{3T} \Delta \lambda_3$, and $\Delta \mu_A = \mu_A - \overline{\mu}_A$, $\Delta \mu_B = \mu_B - \overline{\mu}_B$ represent the increments in Lagrange multipliers associated with the normalization constraints.

Now, let us turn our attention to the Lagrange multipliers μ_A and μ_B. The penalty method allows one to formulate the following relations

$$h_A(\mathbf{q}_A, \mu_A) \equiv \Delta \mu_A - \alpha \Psi_A(\mathbf{q}_A) = 0, \quad h_B(\mathbf{q}_B, \mu_B) \equiv \Delta \mu_B - \alpha \Psi_B(\mathbf{q}_B) = 0, \tag{18}$$

where α is a penalty factor. Equations (18) may be treated as a set of nonlinear algebraic equations in $\mathbf{q}_A$, μ_A and $\mathbf{q}_B$, μ_B as unknowns. Let us expand the relations into a Taylor series by taking the values $(\overline{\mathbf{q}}_A, \overline{\mu}_A)$ and $(\overline{\mathbf{q}}_B, \overline{\mu}_B)$ as operating point, to obtain

$$\Delta \mu_A = \alpha \Psi_{A\mathbf{q}_A}(\overline{\mathbf{q}}_A) \Delta \mathbf{q}_A - h_A(\overline{\mathbf{q}}_A, \overline{\mu}_A), \quad \Delta \mu_B = \alpha \Psi_{B\mathbf{q}_B}(\overline{\mathbf{q}}_B) \Delta \mathbf{q}_B - h_B(\overline{\mathbf{q}}_B, \overline{\mu}_B). \tag{19}$$

Now, if we introduce equations (19) into Eqn. (16) and Eqn. (17), respectively, we obtain almost the final algebraic form useful for further applications.

$$\check{\check{\mathbf{M}}}_A \Delta \mathbf{q}_A + \frac{\Delta t^2}{4} \left(\Delta \mathbf{F}_A^1 + \Delta \mathbf{F}_A^2 \right) = -\frac{\Delta t^2}{4} (\mathbf{g}_A - \Psi_{A\mathbf{q}_A}^T h_A), \tag{20}$$

$$\check{\check{\mathbf{M}}}_B \Delta \mathbf{q}_B + \frac{\Delta t^2}{4} \left(\Delta \mathbf{F}_B^2 + \Delta \mathbf{F}_B^3 \right) = -\frac{\Delta t^2}{4} (\mathbf{g}_B - \Psi_{B\mathbf{q}_B}^T h_B), \tag{21}$$

where $\check{\check{\mathbf{M}}}_A = \check{\mathbf{M}}_A + \frac{\Delta t^2}{4} \Psi_{A\mathbf{q}_A}^T \alpha \Psi_{A\mathbf{q}_A}$ and $\check{\check{\mathbf{M}}}_B = \check{\mathbf{M}}_B + \frac{\Delta t^2}{4} \Psi_{B\mathbf{q}_B}^T \alpha \Psi_{B\mathbf{q}_B}$. Please note that this time the matrices $\check{\check{\mathbf{M}}}_A$, $\check{\check{\mathbf{M}}}_B$ are symmetric and positive definite. Therefore, one can write the following form of discretized equations of motion for body A and B, which is useful in the development of the divide and conquer algorithm:

$$\Delta \mathbf{q}_A = \boldsymbol{\delta}_{i1}^A \Delta \mathbf{F}_A^1 + \boldsymbol{\delta}_{i2}^A \Delta \mathbf{F}_A^2 + \boldsymbol{\delta}_{i3}^A, \quad i = 1, 2, \tag{22}$$

$$\Delta \mathbf{q}_B = \boldsymbol{\delta}_{i1}^B \Delta \mathbf{F}_B^2 + \boldsymbol{\delta}_{i2}^B \Delta \mathbf{F}_B^3 + \boldsymbol{\delta}_{i3}^B, \quad i = 1, 2, \tag{23}$$

where again, for $i = 1, 2$, we get

$$\boldsymbol{\delta}_{i1}^A = \boldsymbol{\delta}_{i2}^A = -\frac{\Delta t^2}{4} \check{\check{\mathbf{M}}}_A^{-1}, \ \boldsymbol{\delta}_{i3}^A = -\frac{\Delta t^2}{4} \check{\check{\mathbf{M}}}_A^{-1} (\mathbf{g}_A - \Psi_{A\mathbf{q}_A}^T h_A), \tag{24}$$

$$\boldsymbol{\delta}_{i1}^B = \boldsymbol{\delta}_{i2}^B = -\frac{\Delta t^2}{4} \check{\check{\mathbf{M}}}_B^{-1}, \ \boldsymbol{\delta}_{i3}^B = -\frac{\Delta t^2}{4} \check{\check{\mathbf{M}}}_B^{-1} (\mathbf{g}_B - \Psi_{B\mathbf{q}_B}^T h_B). \tag{25}$$

Please note, that in general $\boldsymbol{\delta}_{i1}^A \neq \boldsymbol{\delta}_{i2}^A$ and $\boldsymbol{\delta}_{i1}^B \neq \boldsymbol{\delta}_{i2}^B$ for compound bodies considered later in this work. The equality relations are true only for the physical bodies when the assembly process is about to start.

3.2. Generalized formulation

Now, let us generalize the notions made in the previous section for the system of articulated bodies A and B that may be composed of compound bodies as depicted in Fig. 1b. Note that there are three Lagrange multipliers indicated in Fig. 1b. The vectors $\boldsymbol{\lambda}_1$ and $\boldsymbol{\lambda}_2$ correspond to the forces of interaction between the compound body C and the rest of multibody system, whereas constraint loads $\boldsymbol{\lambda}$ represent the forces of interaction between body A and B. Moreover, within each compound body, there are physical bodies marked by numbers 1 and 2.

The discretized form of equations of motion for the representative bodies A and B can be written in the form:

$$\Delta\mathbf{q}_A^1 = \boldsymbol{\delta}_{11}^A \Delta\mathbf{F}_A^1 + \boldsymbol{\delta}_{12}^A \Delta\mathbf{F}_A^2 + \boldsymbol{\delta}_{13}^A, \tag{26}$$

$$\Delta\mathbf{q}_A^2 = \boldsymbol{\delta}_{21}^A \Delta\mathbf{F}_A^1 + \boldsymbol{\delta}_{22}^A \Delta\mathbf{F}_A^2 + \boldsymbol{\delta}_{23}^A, \tag{27}$$

$$\Delta\mathbf{q}_B^1 = \boldsymbol{\delta}_{11}^B \Delta\mathbf{F}_B^1 + \boldsymbol{\delta}_{12}^B \Delta\mathbf{F}_B^2 + \boldsymbol{\delta}_{13}^B, \tag{28}$$

$$\Delta\mathbf{q}_B^2 = \boldsymbol{\delta}_{21}^B \Delta\mathbf{F}_B^1 + \boldsymbol{\delta}_{22}^B \Delta\mathbf{F}_B^2 + \boldsymbol{\delta}_{23}^B. \tag{29}$$

The objective of the first phase of the divide and conquer algorithm, called assembly phase, is to obtain the discretized equations of motion for the compound body C in the form:

$$\Delta\mathbf{q}_C^1 = \boldsymbol{\delta}_{11}^C \Delta\mathbf{F}_C^1 + \boldsymbol{\delta}_{12}^C \Delta\mathbf{F}_C^2 + \boldsymbol{\delta}_{13}^C, \quad \Delta\mathbf{q}_C^2 = \boldsymbol{\delta}_{21}^C \Delta\mathbf{F}_C^1 + \boldsymbol{\delta}_{22}^C \Delta\mathbf{F}_C^2 + \boldsymbol{\delta}_{23}^C. \tag{30}$$

The Lagrange multipliers $\boldsymbol{\lambda}$ associated with the constraint forces between body A and B can be found by using the penalty method:

$$\mathbf{h}_{AB}(\mathbf{q}_A^2, \mathbf{q}_B^1, \boldsymbol{\lambda}) = \Delta\boldsymbol{\lambda} - \alpha\boldsymbol{\Phi}(\mathbf{q}_A^2, \mathbf{q}_B^1) = \mathbf{0}. \tag{31}$$

One can treat Eq. (31) as a set of nonlinear equations in terms of $\mathbf{q}_A^2$, $\mathbf{q}_B^1$, $\boldsymbol{\lambda}$. By expanding Eq. (31) into a Taylor series and neglecting higher order terms, we get

$$\frac{1}{\alpha}\Delta\boldsymbol{\lambda} = \boldsymbol{\Phi}_{\mathbf{q}_A^2}\Delta\mathbf{q}_A^2 + \boldsymbol{\Phi}_{\mathbf{q}_B^1}\Delta\mathbf{q}_B^1 - \frac{1}{\alpha}\overline{\mathbf{h}}_{AB}, \tag{32}$$

where $\overline{\mathbf{h}}_{AB} = \mathbf{h}(\overline{\mathbf{q}}_A^2, \overline{\mathbf{q}}_B^1, \overline{\boldsymbol{\lambda}})$. Then, substituting Eqn. (27) and Eqn. (28) into Eqn. (32) with the addition of Eqn. (12) the following relation that corresponds to the increment of the Lagrange multipliers at considered joint is obtained

$$\Delta\boldsymbol{\lambda} = \mathbf{C}\boldsymbol{\Phi}_{\mathbf{q}_A^2}\boldsymbol{\delta}_{21}^A \Delta\mathbf{F}_A^1 + \mathbf{C}\boldsymbol{\Phi}_{\mathbf{q}_B^1}\boldsymbol{\delta}_{12}^B \Delta\mathbf{F}_B^2 + \mathbf{C}\boldsymbol{\beta}, \tag{33}$$

where $\mathbf{C} = \left(\frac{1}{\alpha}\mathbf{I} - \boldsymbol{\Phi}_{\mathbf{q}_A^2}\boldsymbol{\delta}_{22}^A\boldsymbol{\Phi}_{\mathbf{q}_A^2}^T - \boldsymbol{\Phi}_{\mathbf{q}_B^1}\boldsymbol{\delta}_{11}^B\boldsymbol{\Phi}_{\mathbf{q}_B^1}^T\right)^{-1}$ and $\boldsymbol{\beta} = \boldsymbol{\Phi}_{\mathbf{q}_A^2}\boldsymbol{\delta}_{23}^A + \boldsymbol{\Phi}_{\mathbf{q}_B^1}\boldsymbol{\delta}_{13}^B - \frac{1}{\alpha}\overline{\mathbf{h}}_{AB}$. Please note that the inversion of matrix $\mathbf{C}$ exists, even in the case when constraint Jacobian matrices become rank deficient. Equation (33) is substituted back to Eqns. (26) and (29) to obtain the forms (30). The unknown matrix coefficients are obtained as

$$\boldsymbol{\delta}_{11}^C = \boldsymbol{\delta}_{11}^A + \boldsymbol{\delta}_{12}^A\boldsymbol{\Phi}_{\mathbf{q}_A^2}^T\mathbf{C}\boldsymbol{\Phi}_{\mathbf{q}_A^2}\boldsymbol{\delta}_{21}^A, \tag{34}$$

$$\boldsymbol{\delta}_{12}^C = (\boldsymbol{\delta}_{21}^C)^T = \boldsymbol{\delta}_{12}^A\boldsymbol{\Phi}_{\mathbf{q}_A^2}\mathbf{C}\boldsymbol{\Phi}_{\mathbf{q}_B^1}\boldsymbol{\delta}_{12}^B, \tag{35}$$

$$\boldsymbol{\delta}_{22}^C = \boldsymbol{\delta}_{22}^B + \boldsymbol{\delta}_{21}^B\boldsymbol{\Phi}_{\mathbf{q}_B^1}^T\mathbf{C}\boldsymbol{\Phi}_{\mathbf{q}_B^1}\boldsymbol{\delta}_{12}^B, \tag{36}$$

$$\boldsymbol{\delta}_{13}^C = \boldsymbol{\delta}_{13}^A + \boldsymbol{\delta}_{12}^A\boldsymbol{\Phi}_{\mathbf{q}_A^2}^T\mathbf{C}\boldsymbol{\beta}, \quad \boldsymbol{\delta}_{23}^C = \boldsymbol{\delta}_{23}^B + \boldsymbol{\delta}_{21}^B\boldsymbol{\Phi}_{\mathbf{q}_B^1}^T\mathbf{C}\boldsymbol{\beta}. \tag{37}$$

The divide and conquer algorithm developed here is composed of two computational stages: assembly and disassembly phase. Each phase is associated with the binary tree, which represents the topology of the mechanism (see [2, 8, 16]). The first phase starts with the evaluation of matrix coefficients for individual bodies as in Eqn. (24) and Eqn. (25). Then, the multibody system is assembled. The coefficients in Eqns. (34)–(37) form recursive formulae for coupling two compound bodies A and B into one subassembly C by eliminating the constraint force between them. The process may be repeated and applied for all bodies that are included in the specified subset of bodies up to the moment when the whole MBS is constructed. Finally, a single assembly is obtained. This entity constitutes a representation of the entire multibody system modeled as a single assembly. The first phase finishes at this stage. Taking into account the boundary conditions, e.g., a connection of a chain to a fixed base body and a free floating terminal body, the second phase is started. At this stage all constraint forces increments $\Delta\boldsymbol{\lambda}$ and bodies' positions $\Delta\mathbf{q}$ are calculated according to the binary tree.
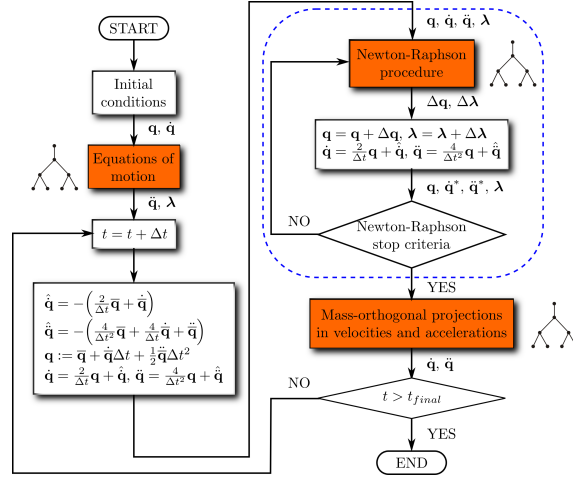
Figure 2: Flowchart of the algorithm. The orange boxes indicate the possiblity to parallelize the computations according to the binary tree associated with topology of a multibody system

3.3. Mass-orthogonal projections

In the previous section we imposed the constraint equations only at the position level. Therefore, it is expected that the first and second derivatives of constraint equations as in Eqn. (2) and Eqn. (3) will not be satisfied during the simulation. To circumvent this effect, mass-orthogonal projections at the velocity and acceleration level are employed [21, 22]. Usually this procedure is numerically expensive due to the iterative scheme involved in the calculations. For real-time applications, one needs a deterministic response. The mass-orthogonal projections are performed only once per integration step, just after the Newton-Raphson procedure converges to the solution.

Fortunately, the calculations associated with projections can be organized in the same divide and conquer manner that is presented in the previous subsection. Moreover, there is a place for many computational savings. In the current stage there is no need to calculate again the matrices $\boldsymbol{\delta}_{11}$, $\boldsymbol{\delta}_{12}$, $\boldsymbol{\delta}_{21}$, and $\boldsymbol{\delta}_{22}$ as defined in Eqns. (34)–(36). The qualitative and quantitative difference between mass-orthogonal projections scheme and the divide and conquer based Newton-Raphson procedure lies in the definitions of $\boldsymbol{\delta}_{13}$, and $\boldsymbol{\delta}_{23}$ coefficients and the involved Lagrange multipliers. Let us assume that the values $\dot{\mathbf{q}}^*$ and $\ddot{\mathbf{q}}^*$ represent the perturbed vectors for which the constraint equations $\dot{\boldsymbol{\Phi}}$, $\ddot{\boldsymbol{\Phi}}$ are not completely satisfied after the convergence of the Newton-Raphson scheme. The following equations respresent one-shot mass-orthogonal projections, in which the constraints $\dot{\boldsymbol{\Phi}}$, $\ddot{\boldsymbol{\Phi}}$ are enforced by the penalty method:

$$\check{\mathbf{g}}_{VEL} \equiv \check{\mathbf{M}}\dot{\mathbf{q}} + \frac{\Delta t^2}{4}\left(\boldsymbol{\Phi}_{\mathbf{q}}^T\boldsymbol{\sigma} + \boldsymbol{\Psi}_{\mathbf{q}}^T\boldsymbol{\sigma}_N\right) - \check{\mathbf{M}}\dot{\mathbf{q}}^* = \mathbf{0}, \tag{38}$$

$$\mathbf{h}_{VEL}^N \equiv \boldsymbol{\sigma}_N - \alpha\boldsymbol{\Psi}_{\mathbf{q}}\dot{\mathbf{q}} = \mathbf{0}, \quad \mathbf{h}_{VEL} \equiv \boldsymbol{\sigma} - \alpha\dot{\boldsymbol{\Phi}} = \boldsymbol{\sigma} - \alpha\boldsymbol{\Phi}_{\mathbf{q}}\dot{\mathbf{q}} = \mathbf{0}, \tag{39}$$

$$\check{\mathbf{g}}_{ACC} \equiv \check{\mathbf{M}}\ddot{\mathbf{q}} + \frac{\Delta t^2}{4}\left(\boldsymbol{\Phi}_{\mathbf{q}}^T\boldsymbol{\kappa} + \boldsymbol{\Psi}_{\mathbf{q}}^T\boldsymbol{\kappa}_N\right) - \check{\mathbf{M}}\ddot{\mathbf{q}}^* = \mathbf{0}, \tag{40}$$

$$\mathbf{h}_{ACC}^N \equiv \boldsymbol{\kappa}_N - \alpha(\boldsymbol{\Psi}_{\mathbf{q}}\ddot{\mathbf{q}} - \boldsymbol{\eta}) = \mathbf{0}, \quad \mathbf{h}_{ACC} \equiv \boldsymbol{\kappa} - \alpha\ddot{\boldsymbol{\Phi}} = \boldsymbol{\kappa} - \alpha(\boldsymbol{\Phi}_{\mathbf{q}}\ddot{\mathbf{q}} - \boldsymbol{\gamma}) = \mathbf{0}, \tag{41}$$

where $\check{\mathbf{M}} = \mathbf{M} - \frac{\Delta t}{2}\frac{\partial \mathbf{Q}}{\partial \mathbf{q}} - \frac{\Delta t^2}{4}\frac{\partial \mathbf{Q}}{\partial \dot{\mathbf{q}}}$ and the Lagrange multipliers $\boldsymbol{\sigma}$, $\boldsymbol{\sigma}_N$ and $\boldsymbol{\kappa}$, $\boldsymbol{\kappa}_N$ are associated with joint and normalization constraints at the velocity and acceleration level, respectively. There are two important things to notice about Eqns. (38)–(41). Firstly, these equations represent a global form of the mass-orthogonal projections that could be expanded to the relations for individual or compound bodies. Secondly, there is a structural similarity between these equations and the discretized equations of motion developed in the previous section (see e.g. Eqn. (16), (18), and (31) for direct comparisons). The correspondence manifests itself in the same mass matrices $\check{\mathbf{M}}$ and Jacobian matrices $\boldsymbol{\Phi}_{\mathbf{q}}$, $\boldsymbol{\Psi}_{\mathbf{q}}$ but different Lagrange multipliers and forcing terms. Figure 2 presents the flowchart of the algorithm. The most computationaly intensive parts the formulation are marked in orange boxes. These procedures may be parallelized by using the approach prosposed in the paper according to the binary tree associated with topology.

4. Numerical test cases

This section presents the results of the numerical simulations of two test cases. The sample mechanisms are chosen intentionally to demonstrate the performance of the formulation in case of modeling of multibody systems possessing

(a) Spatial double pendulum; joints 1 and 2 are spherical   (b) Planar four-bar mechanism; joints 1 – 4 are revolute

Figure 3: Sample test cases

various topologies. The first test case, depicted in Fig. 3a , is a spatial multi-rigid body pendulum. It consists of two bodies interconnected by spherical joint. Moreover, body A is also connected to the base body 0 by spherical joint. This system is an example of open-loop topology. The second test case, presented in Fig. 3b, is a planar four-bar mechanism but modeled as a spatial one. The system exemplifies a closed-loop topology. Particular concerns for simulations of such systems are associated with constraint violation errors as well as modeling issues (redundant constraints or singular configurations). All bodies are modeled as rigid moving either in three dimensions as in case of double pendulum or in the plane as in case of the four-bar mechanism. The length of each body in the systems is 1 meter, mass $1kg$ and inertia matrix equals to $\mathbf{J}' = diag(1.0)kgm^2$ with respect to the axes of appropriate centroidal coordinate frames. Long-time simulations are carried out, with the mechanisms released from the initial state shown in the figures under the gravity forces. The outcome is verified and compared against the numerical values obtained by using commercial multibody solver.

4.1. Spatial double pendulum

Let us consider an open-loop multibody system shown in Fig. 3a. The system is composed of two bodies A and B. The bodies are interconnected by spherical joints 1 and 2. The gravity force acts in the negative direction of y_0 axis. Initially, body A is located along x_0 axis, whereas body B is situated in the x_0z_0 plane and it is pointing at the z_0 direction. Moreover the axes of centroidal coordinate frames $(x_Ay_Az_A)$ and $(x_By_Bz_B)$ are coincident with the global reference frame axes $(x_0y_0z_0)$. As mentioned before the state of the system is described by the set of absolute coordinates. At the initial time instant the Cartesian position of body A and B in the global reference frame $(x_0y_0z_0)$ are given as $\mathbf{r}_A = \begin{bmatrix} 0.5 & 0.0 & 0.0 \end{bmatrix}^T$, $\mathbf{r}_B = \begin{bmatrix} 1.0 & 0.0 & 0.5 \end{bmatrix}^T$, respectively. The linear and angular velocities of the bodies are set to zero. The penalty coefficient for the proposed approach is chosen as $\alpha = 10^6$. The maximum number of iterations in the Newton-Raphson procedure is limited to three, whereas the stop criterion for the procedure is selected to be $||\Delta\mathbf{q}|| < \varepsilon = 10^{-9}$. The time step for the trapezoidal integration rule is constant and equals to $\Delta t = 0.005sec$ while the simulation time is set to be $10sec$.

Figure 4a presents positions of body A and the components of the constraint force at joint 1. The continuous lines in the plots indicate the outcome obtained by the proposed method. Circle marks represent the results produced by commercial multibody software MSC.ADAMS. Dynamic motion of the mechanism is well reproduced by the proposed method and matches the results obtained in ADAMS. On the other hand Fig. 4b demonstrates the constraint violation errors and the total energy of the system. These time plots can be regarded as a kind of performance measures for the proposed approach. At each time instant the constraint violation error shows the norm of joint constraint equations as well as mathematical constraint equations. The total mechanical energy is a sum of kinetic energy and potential energy of the system. The results are bounded. The constraint violations are kept under control with reasonable accuracy compared to the characteristic length of each body ($L = 1m$). The position constraint violation errors are fulfilled with the highest accuracy compared to the errors committed at the velocity or at the acceleration level. This is an expected outcome since the absolute positions are primary variables in the formulation. The total energy of the system is well conserved within the range of the simulation time. It is kept constant and it is approximately equal to zero due to the assumed initial conditions. The behavior of the curve for longer simulation scenarios has a tendency to reduce the total energy of the system.
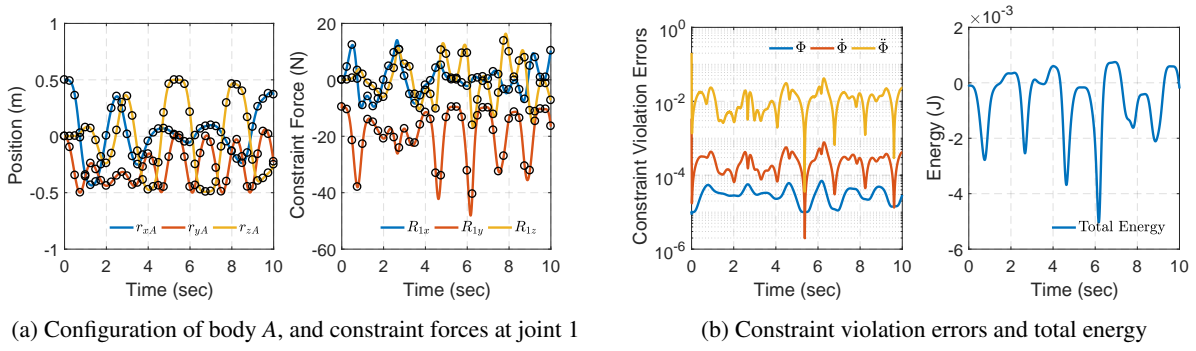
(a) Configuration of body *A*, and constraint forces at joint 1

(b) Constraint violation errors and total energy

Figure 4: Numerical results for the spatial double pendulum

4.2. Four-bar mechanism

This test case is more complex than the first example. The four-bar mechanism is one of the simplest representatives of closed-loop systems. The initial system configuration and topology are presented in Fig. 3b . The mechanism consists of three bodies *A*, *B*, and *C*. The bodies are interconnected to each other and the base body 0 by revolute joints 1–4. Each of these joints has five constraint equations, giving 20 constraint equations. In addition, three Euler parameter normalization constraints yield a total of 23 constraint equations. If absolute coordinates are used, there are 21 generalized coordinates for the three bodies. Since the mechanism possesses one degree of freedom, there must be three redundant constraints. Such over-constrained systems represent a challenge for numerical algorithms. In this situation one has to permanently deal with rank-deficient constraint Jacobian matrices. The existence of redundant constraints might have consequences in non-uniqueness of constraint reactions [27]. The other issue corresponds to a singular configuration. It is encountered when a multibody system reaches a position, in which there is a sudden change in the number of degrees of freedom. For instance, a four-bar mechanism shown in Fig. 3b reaches a singular configuration when the characteristic angle is $\varphi = 90°$ and the links *B* and *C* are overlapped. At this particular state, the constraint equations become dependent and the constraint Jacobian matrix temporarily loses its rank. At this point, the mechanism can theoretically take two different paths (bifurcation point). When the mechanism passes through the neighborhood of the singular configuration, large errors may be introduced into the solution or the simulation may completely fail. The exemplary four-bar mechanism may lose the Jacobian matrix row rank both ways.

Let us assume that initially, the characteristic angle for the four-bar mechanism is $\varphi = 45°$. This angle corresponds to the Cartesian position of the system as depicted in Fig. 3a. It is assumed that initial linear and angular velocities are set to zero. The gravity force is taken as acting in the negative y_0 direction. The simulation time is 10 seconds with the integrator time-step $\Delta t = 0.005 sec$. The time-step is larger than that assumed in the previous example due to the convergence problems. The simulaton parameters are chosen to be $\alpha = 10^6$, $||\Delta \mathbf{q}|| < \varepsilon = 10^{-9}$, and the number of iterations in the Newton-Raphson procedure equals three. Plots of positions, velocities, accelerations and constraint loads at joint 1 are shown in Fig. 5a. Since the system is conservative, the presented time histories are periodic with a dose of symmetry in the results. No sudden changes in constraint force components occur. The proposed approach delivers the numerical results which match to the outcome achieved by commercial multibody software and indicated by marks in the figures. Figure 5b presents the performance of the algorithm for the simulation that lasts 300 seconds. As in open-loop system case, the method gives bounded response in terms of constraint violation errors as well as in terms of the total energy conservation. The constraint errors are kept under control. The total energy of the system indicates a small oscillatory behavior with the tendency to marginal energy dissipation. The energy dissipation is observed partly due to the mass-orthogonal projections involved in the solution process. It can be noticed that the proposed formulation handles well the system with redundant constraints, which may repeatedly pass through the neighborhood of singular configuration.

5. Summary and conclusions

The equations of motion are formulated in terms of absolute coordinates. A unified form of the algorithm is presented at the position, velocity and acceleration level. The unification manifests itself in the computational savings, because the leading matrices at the mentioned levels are evaluated only once per integration step. Also, the employed Euler parameter form of the equations of motion is particularly useful in deriving the divide and conquer algorithm presented in this paper. The associated mass matrix is invertible and the derived divide and conquer formulae are simpler. The equations of motion for the spatial multi-rigid body system dynamics are discretized by using a single-step trapezoidal rule as an integration scheme. The employed framework leads to the set of nonlinear algebraic equations for the bod-

(a) Configuration of body *A*, and constraint forces at joint 1   (b) Constraint violation errors and total energy
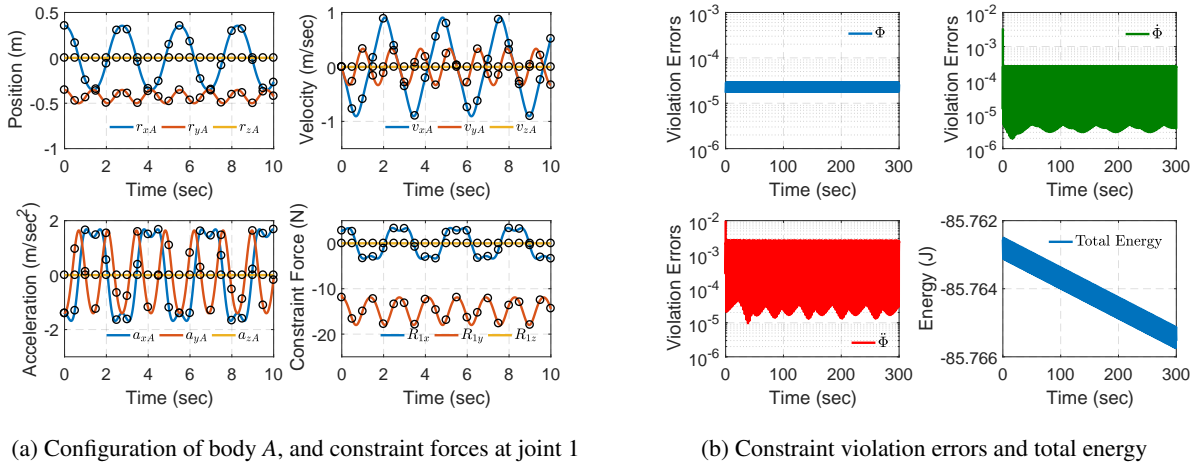
Figure 5: Numerical results for the fourbar mechanism

ies' positions and for the Lagrange multipliers associated with constraint equations. These equations are solved by the Newton-Raphson procedure with the add of the second order predictor. It is assumed that the constraint equations for multibody systems are imposed at the position level. In consequence, one may expect the accumulation of constraint errors for velocities and accelerations. To correct the constraint violation errors, the resulting classical index-3 formulation is supplemented by the two mass-orthogonal projections.

The robustness of the formulation manifests itself in the ability of the algorithm to analyze multibody systems with redundant constraints, and the systems that may occasionally enter into singular configurations. The problems associated with such systems are reflected in numerical difficulties, and in some situations, inability of the algorithm to continue the simulation as reported. The proposed algorithm circumvents the problems by introducing the approximations of Lagrange multipliers. The key matrices in the formulation remain nonsingular, and simultaneously, the constraint equations are fulfilled within the reasonable accuracy dependent on the tolerance imposed in the calculations. Due to the necessity of the solution of nonlinear equations of motion, the proposed formulation is inherently iterative. The largest computational load is associated with iterations performed by the Newton-Raphson algorithm, where the increments in positions and Lagrange multipliers are evaluated to predict the state of the system in the next time-instant. The computational burden can be reduced each next iteration by assuming that the tangent matrix in the Newton-Raphson procedure is constant. On the other hand, the error corrections at the velocity and acceleration level are performed only once per integration step. The mass-orthogonal projections based procedures make use of the tangent matrix evaluated in the Newton-Raphson procedure. In fact, the numerical cost associated with the projections is only a part of the burden required in the first iteration of the Newton-Raphson scheme.

Finally, the divide and conquer scheme is employed on top of the index-3 formulation with mass-orthogonal projections. The trapezoidal rule is embedded into the solution process without the deterioration of the binary-tree structure of the algorithm. This notion can be extended for incorporation of various structural integrators available in the literature. The proposed approach enables one to parallelize the involved computations at the position, velocity and acceleration levels. The efficiency gains can be obtained for the simulation of large multibody systems. The overall wall-clock time associated with the simulations can be further diminished by careful implementations on various embedded platforms as well as parallel computers involving multicore processor units or/and graphical processor units.

Acknowledgments

References

[1] D. Negrut, R. Serban, H. Mazhar, and T. Heyn, "Parallel computing in multibody system dynamics: Why, when, and how," *Journal of Computational and Nonlinear Dynamics*, vol. 9, no. 4, 2014.

[2] R. Featherstone, "A divide–and–conquer articulated–body algorithm for parallel O(log(n)) calculation of rigid–body dynamics." *The International Journal of Robotics Research*, vol. 18, pp. 867–875, 1999.

[3] I. M. Khan and K. S. Anderson, "A logarithmic complexity divide-and-conquer algorithm for multi-flexible-body dynamics including large deformations," *Multibody System Dynamics*, vol. 34, no. 1, pp. 81–101, 2015.

[4] J. J. Laflin, K. S. Anderson, I. M. Khan, and M. Poursina, "Advances in the application of the dca algorithm to multibody system dynamics," *Journal of Computational and Nonlinear Dynamics*, vol. 9, no. 4, 2014.

[5] R. M. Mukherjee and K. S. Anderson, "Orthogonal complement based divide–and–conquer algorithm for constrained multibody systems," *Nonlinear Dynamics*, vol. 48, pp. 199–215, 2007.

[6] M. Poursina and K. S. Anderson, "An extended divide-and-conquer algorithm for a generalized class of multibody constraints," *Multibody System Dynamics*, vol. 29, no. 3, pp. 235–254, 2013.

[7] R. M. Mukherjee and K. S. Anderson, "A logarithmic complexity divide-and-conquer algorithm for multi-flexible articulated body dynamics," *Journal of Computational and Nonlinear Dynamics*, vol. 2, no. 1, pp. 10–21, 2006.

[8] ——, "Efficient methodology for multibody simulations with discontinuous changes in system definition," *Multibody System Dynamics*, vol. 18, no. 2, pp. 145–168, 2007.

[9] K. D. Bhalerao, K. S. Anderson, and J. C. Trinkle, "A recursive hybrid time-stepping scheme for intermittent contact in multi-rigid-body dynamics," *Journal of Computational and Nonlinear Dynamics*, vol. 4, no. 4, 2009.

[10] I. M. Khan and K. S. Anderson, "Performance investigation and constraint stabilization approach for the orthogonal complement-based dca," *Mechanism and Machine Theory*, vol. 67, pp. 111–121, 2013.

[11] R. Mukherjee and P. Malczyk, "Efficient approach for constraint enforcement in constrained multibody system dynamics," in *ASME 2013 IDETC/CIE Conferences, International Conference on Multibody Systems, Nonlinear Dynamics, and Control*, Portland, Oregon, USA, 2013, pp. 1–8.

[12] J. H. Critchley, K. S. Anderson, and A. Binani, "An efficient multibody divide and conquer algorithm and implementation," *Journal of Computational and Nonlinear Dynamics*, vol. 4, no. 2, 2009.

[13] M. Poursina, K. D. Bhalerao, S. C. Flores, K. S. Anderson, and A. Laederach, "Strategies for articulated multibody-based adaptive coarse grain simulation of RNA," *Methods in Enzymology*, vol. 487, pp. 73–98, 2011.

[14] P. Malczyk and J. Frączek, "Molecular dynamics simulation of simple polymer chain formation using divide and conquer algorithm based on the augmented lagrangian method," *Proceedings of the Institution of Mechanical Engineers, Part K: Journal of Multi-body Dynamics*, vol. 2, no. 229, pp. 116–131, 2015.

[15] R. Featherstone, "The calculation of robot dynamics using articulated-body inertias," *The International Journal of Robotics Research*, vol. 2, no. 1, pp. 13–30, 1983.

[16] K. D. Bhalerao, J. Critchley, and K. Anderson, "An efficient parallel dynamics algorithm for simulation of large articulated robotic systems," *Mechanism and Machine Theory*, vol. 53, pp. 86–98, 2012.

[17] K. Chadaj, P. Malczyk, and J. Frączek, "A parallel recursive hamiltonian algorithm for forward dynamics of serial kinematic chains," *IEEE Transactions on Robotics*, vol. 33, no. 3, pp. 1–14, 2017.

[18] ——, "A parallel hamiltonian formulation for forward dynamics of closed-loop multibody systems," *Multibody System Dynamics*, vol. 1, no. 39, pp. 51–77, 2017.

[19] P. Malczyk and J. Frączek, "A divide and conquer algorithm for constrained multibody system dynamics based on augmented Lagrangian method with projections-based error correction," *Nonlinear Dynamics*, vol. 70, no. 1, pp. 871–889, 2012.

[20] E. Bayo, J. García de Jalón, and M. A. Serna, "A modified Lagrangian formulation for the dynamic analysis of constrained mechanical systems," *Computer Methods in Applied Mechanics and Engineering*, vol. 71, no. 2, pp. 183–195, 1988.

[21] E. Bayo and R. Ledesma, "Augmented Lagrangian and mass–orthogonal projection methods for constrained multibody dynamics," *Nonlinear Dynamics*, vol. 9, no. 1-2, pp. 113–130, 1996.

[22] J. Cuadrado, J. Cardenal, and E. Bayo, "Modeling and solution methods for efficient real-time simulation of multibody dynamics," *Multibody System Dynamics*, vol. 1, no. 3, pp. 259–280, 1997.

[23] J. Cuadrado, J. Cardenal, P. Morer, and Bayo, "Intelligent simulation of multibody dynamics: Space–state and descriptor methods in sequential and parallel computing environments," *Multibody System Dynamics*, vol. 4, no. 1, pp. 55–73, 2000.

[24] D. Dopico, F. González, J. Cuadrado, and J. Kövecses, "Determination of holonomic and nonholonomic constraint reactions in an index-3 augmented Lagrangian formulation with velocity and acceleration projections," *Journal of Computational and Nonlinear Dynamics*, vol. 9, no. 4, 2014.

[25] D. Dopico, A. Luaces, M. González, and J. Cuadrado, "Dealing with multiple contacts in a human-in-the-loop application," *Multibody System Dynamics*, vol. 25, no. 2, pp. 167–183, 2011.

[26] P. Malczyk, J. Frączek, and J. Cuadrado, "Parallel index-3 formulation for real-time multibody dynamics simulations," in *Proc. of the 1st Joint IMSD Conference, Lappeenranta, Finland*, Lappeenranta, Finland, 2010.

[27] M. Wojtyra and J. Frączek, "Comparison of selected methods of handling redundant constraints in multibody systems simulations," *Journal of Computational and Nonlinear Dynamics*, vol. 2, no. 8, 2013.